

## Comparison of Analytical and Numerical Models on Torque and Hookload Calculation

Andrew Wu

Schulich School of Engineering, University of Calgary  
2500 University Drive NW, Calgary, T2N 1N4, Canada

Geir Hareland

Schulich School of Engineering, University of Calgary  
2500 University Drive NW, Calgary, T2N 1N4, Canada

Mohammad Fazelizadeh

Schulich School of Engineering, University of Calgary  
2500 University Drive NW, Calgary, T2N 1N4, Canada

**Abstract:** An analytical model for drillstring torque and drag is generated using a soft model. The soft model does not integrate all parameters affecting the drillstring behavior although some other researchers have taken the stiffness into account in the soft model. The torque and drag calculated by finite element method (FEM) is more accurate than the analytical model. The FEM can generate results that the analytical method cannot. This is because that the FEM takes both stiffness and some complicated boundary conditions into account.

The program developed and presented in this paper can be used for torque and drag analysis in vertical, directional, horizontal, and other complicated wells under different drilling operational modes.

Three examples on the calculation of torque and hookload are presented. The comparison between the analytical and numerical models was done, and the results were also compared with field data. The comparison shows that the result from FEM in one example matches the field data well but the analytical model doesn't get good results no matter how the friction coefficient is adjusted.

The calculation of the contact force between the drillstring and the wellbore wall was conducted using the FEM. The calculated contact force estimates where the contact happens, as well as brings information about the location of possible drillstring sticking. The analytical model cannot do this, because the entire drillstring is in contact with the low side of the hole.

The FEM program presented in this paper will enforce real-time analysis correctness of torque and drag together with the analytical model. The value of these torque and drag models could play an important role in real-time and planning of future drilling operations.

### INTRODUCTION

In 1983, Johancsic developed a drillstring torque and drag model for directional wells where the drillstring is modeled as a cable with weight but no stiffness. The model operates by calculating the normal force on the lowest element of the drillstring, computing the incremental tension and torque, and then applying this to the next element above. This continues to the top of the drillstring[1]. Based on the above model, many researchers (Aadnoy, 2010, and M. Fazelizadeh, 2010) have done practical application analysis and simulation[2, 3]. Since the model ignores the effects of drillstring bending stiffness on wall-contact forces, it is unable to perform some of the more sophisticated calculations in more challenging well bores. There have been many stiff string models developed, but there is no industry standard [4]. The rapid advance of computing power and the even more spectacular reduction in computing cost has subsequently led to more widespread use of Finite Element Analysis (FEA). The Finite Element Method (FEM) has been used for a number of years in the oilfield [5]. The basic concept is to subdivide a large complex structure into a finite number of sample elements, such as beam, plate, and shaft elements. In this case, a set of  $n$  second-order differential equations are obtained where  $n$  is the number of discretized degrees of freedom [6]. Therefore no matter how complicated the wellbore curvature, the drillstring and the boundaries are, FEM can get the solution. The drillstring is meshed into beam elements, each of which has six degrees of freedom (three

rotations and three displacements). The only shortcoming is that it is time consuming when the number of elements is large. It is interesting to note that finite element procedures have been used to study the drill-strings for some time but most studied only the Bottom-Hole-Assemblies, BHA. Yang D. presents a three-dimensional finite difference differential method for bottomhole assembly (BHA) analysis under static loads. The analysis was to optimize the BHA configurations for drilling directional boreholes. The model incorporates the contact response between drillstring and wellbore wall, the upper tangent point, stabilizer configurations, bent sub model and other considerations for numerical solutions[7]. Piovani made the nonlinear analysis of the coupling of extensional, flexural and torsional vibrations on a drillstring by means of finite element discretization, however the drillstring is limited to a vertical well[8]. Zhu etc. developed a complete model that describes the behavior of drill string in a 3d wellbore, considering all boundaries including fluid effect, rotary speed effect, interaction of drillstring and wellbore wall, interaction of drill bit and bottom rock. However, no more detailed applications on torque and drag are seen from that FEA model [9].

This paper briefly introduces the common analytical model and a practical FEA model that can reflect drill string behavior in different modes, including tripping in, tripping out, rotating off bottom, drilling ahead, reaming and back reaming, sliding and 3-D rotary steering drilling. In this paper a few application examples are presented showing comparison between analytical model and FEA model.

### Analytical Model of Torque and Drag

Aadnoy developed a simple model for torque and drag combining axial and rotary motion. During combined motion, the axial velocity is  $V_h$ , and the tangential pipe speed is  $V_r$ , there is a relation (Equation 1) between  $V_h$  and  $V_r$ .

$$\psi = \tan^{-1}\left(\frac{V_h}{V_r}\right) = \tan^{-1}\left(\frac{60V_h(\text{m/s})}{2\pi N_r(\text{rpm})r(\text{m})}\right) \quad \text{Eq.1}$$

For entire straight section, the tension force and torque can be expressed as Equations 2 and 3:

$$F_i = F_{i-1} + \{\beta w \Delta L \cos \alpha\}_i + \{\beta w \Delta L \sin \alpha \times \mu \times \sin \psi\}_i \quad \text{Eq.2}$$

$$T_i = \{\mu \times \beta w \Delta L r \sin \alpha \times \cos \psi\}_i \quad \text{Eq.3}$$

For entire curved section, the tension force and torque can be expressed as Equations 4 and 5:

$$F_i = F_{i-1} + F_{i-1} \times (e^{\pm \mu_i |\theta_i|} - 1) \times \sin \psi_i + \beta_i w_i \Delta L_i \times \left[ \frac{\sin \alpha_i - \sin \alpha_{i-1}}{\alpha_i - \alpha_{i-1}} \right] \quad \text{Eq.4}$$

$$T_i = \mu_i \times r_i F_{i-1} |\theta_i| \times \cos \psi_i \quad \text{Eq.5}$$

### FE Modeling of Drill String

#### Model of FEA

Hamilton's principle is used to derive the following dynamic equation (Equation 6) for an element.

$$[M]^e \{\ddot{U}\}^e + [C]^e \{\dot{U}\}^e + [K]^e \{U\}^e = \{F\}^e \quad \text{Eq.6}$$

Where the vectors  $\{U\}^e$ ,  $\{\dot{U}\}^e$ ,  $\{\ddot{U}\}^e$  and  $\{F\}^e$  represent generalized displacement, velocity, acceleration and force in local coordinate system respectively. The matrix  $\{M\}^e$ ,  $\{C\}^e$  and  $\{K\}^e$  represents element mass, damping and stiffness matrix respectively.

The drillstring is divided into a number of beam elements as shown in Figure 1. Each element has two nodes, and totally 12 degrees of freedom, so the vectors are:

$$\{U\}^e = \{U_1 \quad U_2 \quad U_3 \quad U_4 \quad U_5 \quad U_6 \quad U_7 \quad U_8 \quad U_9 \quad U_{10} \quad U_{11} \quad U_{12}\}^T$$

$$\{\dot{U}\}^e = \{\dot{U}_1 \quad \dot{U}_2 \quad \dot{U}_3 \quad \dot{U}_4 \quad \dot{U}_5 \quad \dot{U}_6 \quad \dot{U}_7 \quad \dot{U}_8 \quad \dot{U}_9 \quad \dot{U}_{10} \quad \dot{U}_{11} \quad \dot{U}_{12}\}^T$$

$$\{\ddot{U}\}^e = \{\ddot{U}_1 \quad \ddot{U}_2 \quad \ddot{U}_3 \quad \ddot{U}_4 \quad \ddot{U}_5 \quad \ddot{U}_6 \quad \ddot{U}_7 \quad \ddot{U}_8 \quad \ddot{U}_9 \quad \ddot{U}_{10} \quad \ddot{U}_{11} \quad \ddot{U}_{12}\}^T$$

$$\{F\}^e = \{F_1 \quad F_2 \quad F_3 \quad F_4 \quad F_5 \quad F_6 \quad F_7 \quad F_8 \quad F_9 \quad F_{10} \quad F_{11} \quad F_{12}\}^T$$

Where the detailed content about  $\{M\}^e$ ,  $\{C\}^e$  and  $\{K\}^e$  will not be discussed in this report. The boundaries include mainly three location constraint: wellhead, stabilizer and drill bit. The element matrix or vectors must be transformed and assembled to global matrix or vectors. A numerical method, Wilson- $\theta$  method, is used to get the solution to the dynamic equations [10].

#### *Torque & drag modeling*

The contact force, or normal force, can be obtained automatically by the finite element method/program, so the axial drag and torque can be obtained easily (Equations 7 and 8) if axial and tangential friction coefficient is given respectively. The friction force and torque on each element can be calculated as follows.

$$F_f = \mu_a \cdot F_n \quad \text{Eq.7}$$

$$T_f = \mu_t \cdot F_n \cdot r \quad \text{Eq.8}$$

### **Applications and Comparison of the Two Models**

#### *Horizontal well drilling example*

Well A and B

There are two horizontal wells. Well A has the following configuration: A 9 5/8" surface casing string was run to 2090 ft. An intermediate 7" casing was set at 7500 ft and then 6 1/8" bit was used for drilling horizontal section to reach the target. The 4 1/2" production casing shoe was set at 10970 ft. The geometry of well B is just like that shown in figure 5.

#### *Extended reach well drilling example*

Well C

This is a more complex example, and a very good example for friction analysis to different sections of well geometry including straight inclined, curved and horizontal sections. The geometry of well B is just like that shown in figure 6 and 7.

#### *Explanations and analysis of results*

Figure 2 indicates that FEA has a closer solution under the normal conditions, because it lies in the middle area of the field data region. Figure 3 also shows that FEA has a closer result than analytical model. The analytical model used a friction coefficient of 0.4, and FEA uses 0.2, which means that the analytical model almost couldn't reach the result like FEA unless a bigger friction coefficient is used (typically values from 0.1 to 0.3 seen). Figure 4 shows that the hook load calculated from the FEA has a better match with the field data than that from the analytical model.

#### *The contact force and WOB's effect*

As mentioned previously, the FEA can get the spatial state of drill string because of the consideration of stiffness and complicated boundaries. The figures 5 and 6 are to show the contact force between drillstring and wellbore in the two wells while running-in and running-out respectively. The figure 7 shows the effect of WOB on the contact force. It can be seen that when WOB increases the contact forces along the drill string also are changed. Because of this the WOB on the surface will change. This is one of reasons that cause the difference between the surface measured SWOB and downhole seen WOB.

### **Conclusions and Recommendations**

1. Three examples show that the results from finite element method are more accurate than those from the analytical model.
2. By considering stiffness in finite element model, the contact surface area could be more realistic

compared to the analytical model which assumes the drill string has full contact with the wellbore. Although the FEA model works well based on the above examples, there is still work needed to integrate it into practical use in the field. The next steps are to find and use more field data to calibrate the model and to use more effective algorithm to reduce calculation time.

### ACKNOWLEDGEMENT

The authors would like to thank NSERC (Natural Sciences and Engineering Research Council of Canada), Talisman Energy Inc. and Pason Systems Corp. for sponsoring this research.

### REFERENCE

- 1) Brett, J.F., Beckett, A.D., Holt, C.A. and Smith, D.L. 1989. Uses and Limitations of Drillstring Tension and Torque Models for Monitoring Hole conditions. SPE Drilling Engineering 4(3):223-229. SPE-16664. doi:10.2118/16664-PA
- 2) Fazelizadeh, M., Hareland, G., and Addnoy, B.S. 2010. Application of New 3-D Analytical Model for Directional Wellbore Friction. Modern Applied Science 4(2):2-22.
- 3) Addnoy, B.S., Fazelizadeh, M. and Hareland, G. 2010. A 3D Analytical Model for Wellbore Friction. Journal of Canadian Petroleum Technology 49(10):25-36. doi: 10.2118/141515-PA
- 4) Mitchell, R.F, and Samuel, R. 2009. How Good Is the Torque/Drag Model? SPE Drilling & Completion: 62-71. SPE-105068. doi:10.2523/105068-MS
- 5) Aslaksen, H., Annand, M., Duncan, R., Fjaere, A., Paez, L. And Tran, U. 2006. Integrated FEA Modeling Offers System Approach to Drillstring Optimization. Paper SPE 99018 presented at the 2006 IADC/SPE Drilling Conference held in Miami, Florida, USA, 21-23 February 2006. doi:10.2523/99018
- 6) Alnaser H.A. 2002. Finite Element Dynamic Analysis of Drillstring. PhD Dissertation, Mechanical Engineering, King Fahd University of Petroleum & Minerals.
- 7) Newman. K.R. and Procter R. 2009. Analysis of Hook Load Forces during Jarring. Paper SPE 118435 presented at the 2009 IADC/SPE Drilling Conference and Exhibition held in Amsterdam, The Netherlands, 17-19 March 2009. doi:10.2118/118435-MS
- 8) Piovan, M. T. and Sampaio, R. 2006. Non Linear Model for Coupled Vibrations of Drill-string. Mecánica Computacional Vol XXV, pp. 1751-1765(2006)
- 9) Zhu, X.H., Liu, Q.Y. and Tong H. 2008. Research on dynamics model of full hole drilling string system with three-dimensional trajectory. Acta Petrolei Sinica, 2008, 29(2) 288-291 DOI: ISSN: 0253-2697 CN: 11-2128/TE
- 10) Wu, A., Hareland, G. and Fazelizadeh, M. 2011. Torque & Drag Analysis Using Finite Element Method. Modern Applied Science: Vol. 5, No. 6, December 2011.

### FIGURES AND DRAWINGS

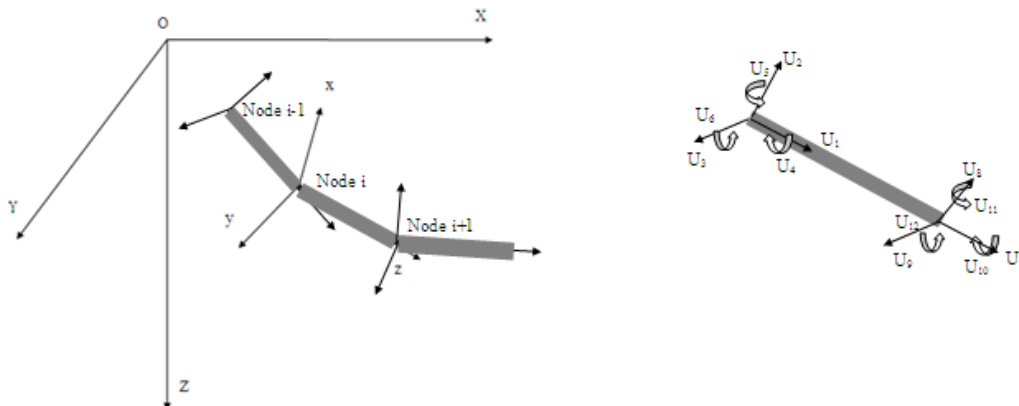


Figure 1: discretization of a drillstring

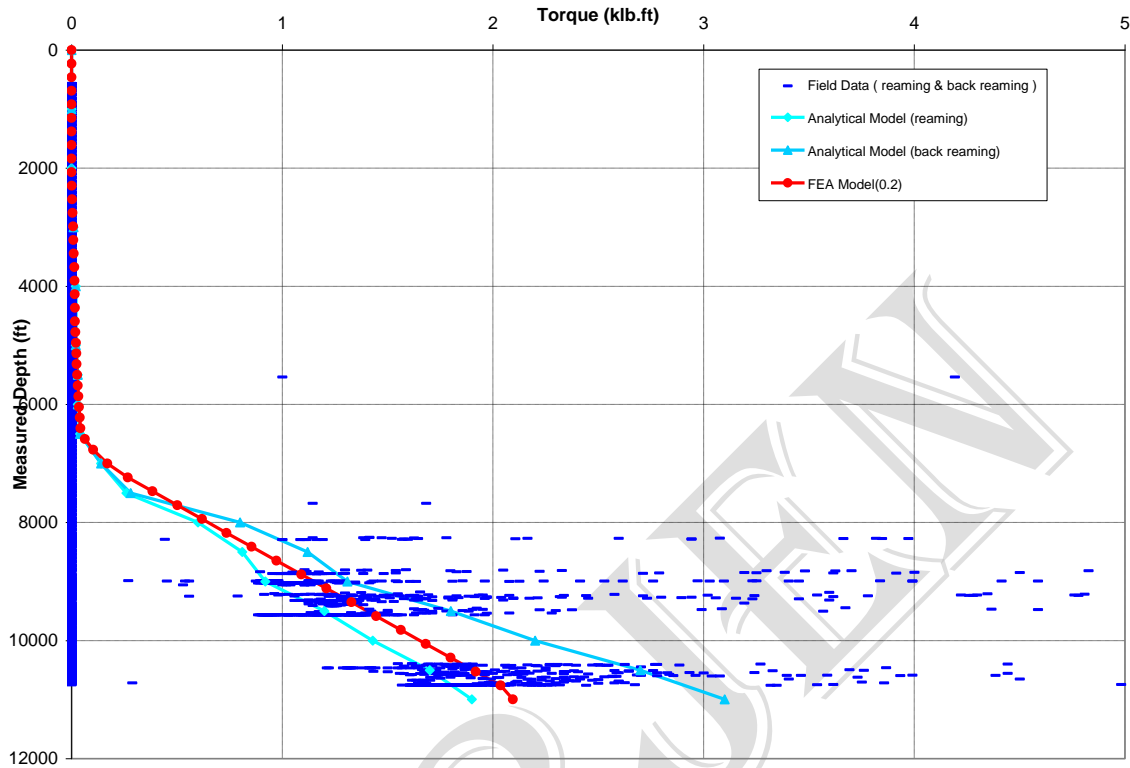


Figure2. The calculated torque versus measured depth (Well A)

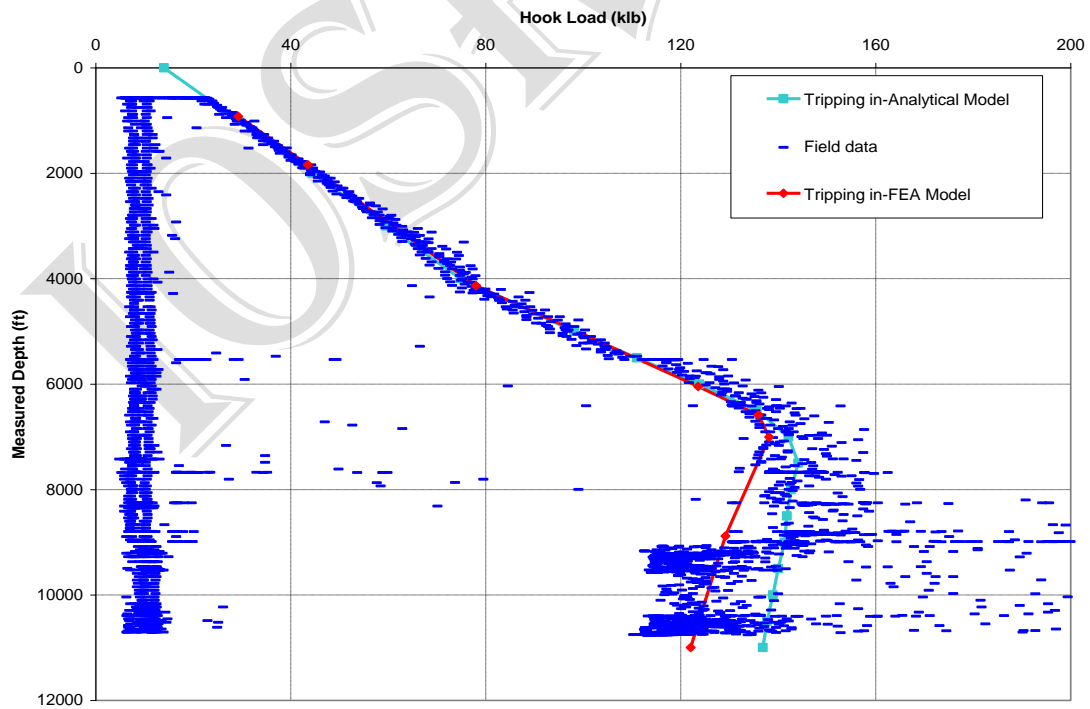


Figure3. The calculated hook load versus measured depth (Well A)

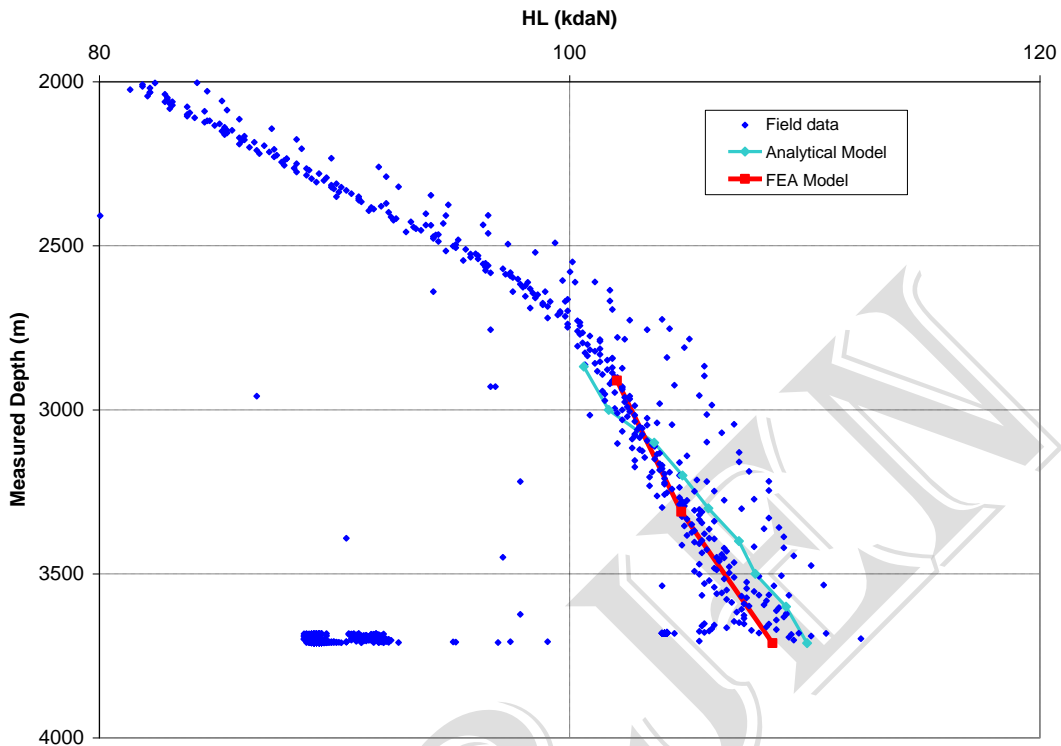


Figure 4: Hookload comparison between the two models (Well B)

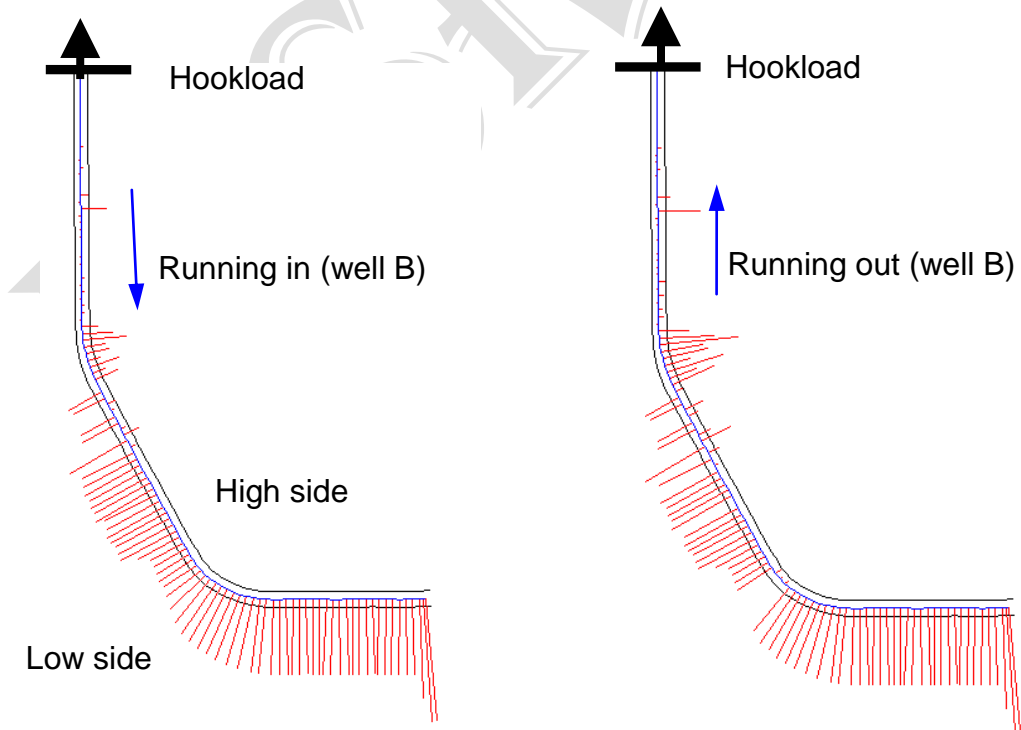


Figure 5: Contact force from the FEA model (well B)

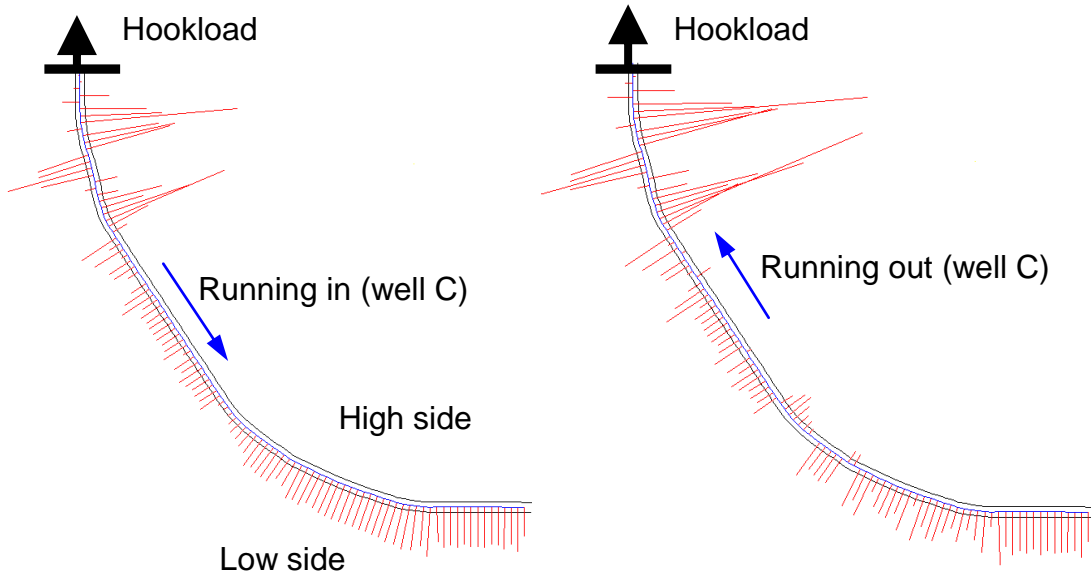


Figure 6: Contact force from the FEA model (well C)

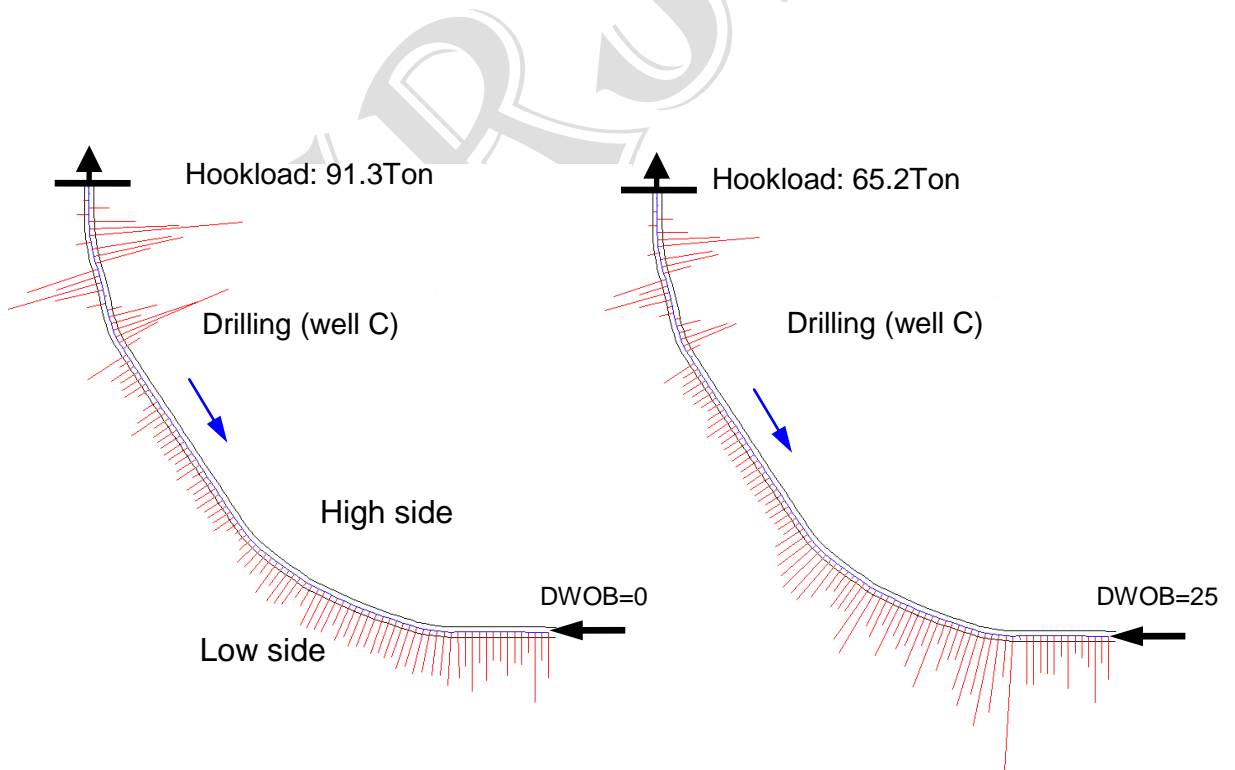


Figure 7: Effect of WOB on contact force from the FEA model (well C)